Express Polymer Letters Vol.16, No.10 (2022) 1083–1098
Available online at www.expresspolymlett.com
https://doi.org/10.3144/expresspolymlett.2022.79

Research article

Physical and antibacterial properties of PLA electrospun mats loaded with carvacrol and nisin

Francesco Lopresti[1], *Luigi Botta*[1*], *Vincenzo La Carrubba*[1], *Giuseppe Attinasi*[2], *Luca Settanni*[2], *Giuliana Garofalo*[2], *Raimondo Gaglio*[2]

[1]Department of Engineering, University of Palermo, RU INSTM, Viale delle Scienze, Palermo, Italy
[2]Dipartimento Scienze Agrarie, Alimentari e Forestali, Università degli Studi di Palermo, Viale delle Scienze 4, 90128 Palermo, Italy

Received 4 March 2022; accepted in revised form 15 June 2022

Abstract. Functional, biopolymeric electrospun structures for the controlled release of antimicrobial agents are gaining increasing interest in food packaging applications. In this study, the physical and antibacterial performances of ternary systems composed of polylactic acid (PLA) electrospun mats loaded with 20 wt% of different relative amounts of carvacrol (CRV) and a commercial nisin formulation (Nis) were assessed. Scanning electron micrographs displayed micro-scaled fibers with different diameter size distributions depending on the relative concentrations of the additives. The PLA/CRV/Nis membranes' wettability was affected by the relative amount of CRV and Nis loaded, switching from hydrophobic to hydrophilic at the highest Nis concentrations. Thermal and tensile tests assessed the plasticizer action of CRV on PLA, while the Nis formulation was found to modify the mechanical behavior of the membranes from ductile to brittle. The release profiles of CRV and Nis from PLA/CRV/Nis structures, assessed via spectroscopical measurements and fitted with a power-law model, permitted to investigate of the different release mechanisms of the additives as a function of their relative concentration. The determination of the antibacterial activity of the electrospun material clearly indicated that the most effective inhibition of food-borne pathogenic bacteria was registered with PLA containing 20% of CRV.

Keywords: *biopolymers, biocomposites, biodegradable polymers, nanomaterials electrospinning, antimicrobial polymers*

1. Introduction

In the last two decades, biopolymers have been widely explored for innovative applications, such as active food packaging [1, 2] and biomedical device fabrication [3]. In this frame, there is a rising interest in functional polymeric porous structures characterized by the ability to release antimicrobial agents in a controlled manner [4, 5].

Due to the possibility of large amounts of drug loading, ease of operation, and cost-effectiveness, electrospinning is an attractive technique for the fabrication of drug delivery systems [6]. Furthermore, the additive incorporation into the polymeric matrices does not require any additional chemical reactions, thus preserving the chemical structure of the drugs [7].

Among the different biopolymeric matrices suitable for the electrospinning process, such as poly(ε-caprolactone), polyethylene glycol [8], and poly(vinyl-alcohol), polylactic acid (PLA) is one of the most extensively investigated to make fibers with desired properties for tissue engineering and drug delivery applications [9, 10].

PLA is an aliphatic polyester, biocompatible and biodegradable at a slow rate, recognized as 'generally recognized as safe' (GRAS) by the U.S. Food and Drug Administration (FDA) for food and biomedical

*Corresponding author, e-mail: luigi.botta@unipa.it

applications [11]. These properties made PLA well-meaning as drug-carrier matrix for biomedical applications and active food packaging [10, 12]. PLA-based electrospun systems were loaded with different kinds of drugs including anti-inflammatory [13, 14], antimicrobial [15–19], anticancer [20–22], cardiovascular drugs [23, 24], and gastrointestinal drugs [25].

In recent years, electrospinning has been gaining more and more attraction for active food packaging applications [26, 27]. Aiming at prolonging the shelf-life of foods, several antimicrobial compounds were investigated as an additive for electrospun systems, including inorganic nanoparticles [28, 29], essential oils (EOs) [30–32], and bacteriocins [33].

In this context, plant-derived EOs are among the most investigated antimicrobial agents for food packaging applications due to their elevated inhibitory potential versus a broad range of microorganisms [34, 35]. The main compound of thyme and oregano EOs is carvacrol (CRV), a monoterpenoid phenol approved by FDA as GRAS food additive [36]. Due to its capacity to prevent undesired spoilage and pathogenic microorganisms, CRV is obtaining increasing acceptance among food scientists [8, 10].

The synergistic antimicrobial action due to the combinations of CRV with other antimicrobial systems such as other EOs [37, 38], ammonium-modified clays [39], and bacteriocins [40, 41] was already reported in the literature. This property allows the lessening of the minimum preservative concentration needed for food preservation, thus decreasing undesirable alterations in their organoleptic and chemophysical properties [41]. Churklam *et al*. [41] observed a synergic antimicrobial action due to the combination of carvacrol and nisin against *L. monocytogenes* on ready-to-eat sliced bologna sausages samples.

Nisin is an antibiotic peptide (lantibiotic), recognized as GRAS by FDA [42] and authorized preservative in the European Union (EU) for use in several food biopreservation strategies [41].

Several research papers deal with including one antimicrobial additive in electrospun membranes for biomedical or, more recently, for active food packaging applications. In this frame, there is a lack of data regarding the controlled release of two antimicrobial additives simultaneously included in an electrospun membrane for active food packaging applications. Recently, our research group demonstrated the efficacy of an antibacterial, biodegradable film loaded with CRV and nisin, fabricated by melt mixing and compression molding [43]. Nevertheless, to the best of our knowledge, the physical and antibacterial properties of an electrospun PLA membrane simultaneously loaded with CRV and nisin were never described so far.

The object of this study is to explore the achievability, the physical and antibacterial performances of PLA electrospun membranes containing CRV, and a commercial formulation of nisin (Nis) designed for food packaging applications. The morphology of the PLA-based materials was assessed via scanning electron microscopy. Water contact angle measurements of PLA/CRV, PLA/Nis, and PLA/CRV/Nis were carried out to assess the wettability of the structures. The mechanical properties of the systems were evaluated by tensile tests. The thermal properties of PLA-based materials were assessed via differential scanning calorimetry, aiming to investigate the effect of the two compounds and their mixture on PLA electrospun fibers. The release profiles of CRV and Nis from PLA-based structures were evaluated via spectroscopical measurements, and they were fitted with a power-law model. The antibacterial activity of the materials containing different relative amounts of CRV and Nis was tested in vitro against the main food-borne pathogenic bacteria.

2. Materials and methods

2.1. Materials

In this work, PLA (Ingeo 2002D, NatureWorks LLC, Minnetonka, MN, USA) was used as the biodegradable polymer matrix. CRV (purity ≥ 98%), acetone (Ac), and chloroforms (TCM) were purchased from Sigma Aldrich, Munich, Germany. In this work, a commercial formulation of nisin (Nisin A, Handary S.A., Brussels, Belgium), hereafter coded as Nis, was used. The formulation contains a concentration of nisin > 2.5 wt% mixed with sodium chloride (>75 wt%) and non-fat dry milk compounds. All the reactants were ACS grade (purity >99%).

2.2. Electrospinning processing

In order to produce the electrospun structures, 10 wt% of PLA was solubilized in a mixture of TCM and Ac (TCM:Ac 2:1 vol) underneath to magnetic stirring overnight, at ambient temperature. PLA/CRV/Nis suspensions were made by loading CRV and/or Nis to the TCM:Ac solvent mixture that was then subjected to magnetic stirring for 1 h needed to obtain a homogeneous dispersion. Thereafter, PLA was added

Table 1. PLA/CRV/Nis formulations and sample codes.

Sample code	CRV [wt%]*	Nis [wt%]*	Nisin [wt%]*
PLA	0	0	0
PLA/CRV/NIS 20/0	20	0	0
PLA/CRV/NIS 15/5	15	5	>0.125
PLA/CRV/NIS 10/10	10	10	>0.25
PLA/CRV/NIS 5/15	5	15	>0.375
PLA/CRV/NIS 0/20	0	20	>0.5

*Concentration with respect to PLA

at 10 wt% with respect to TCM:Ac mixture. The total amount of antimicrobial additives loaded to the solvent mixture was 20 wt% with respect to PLA, although five relative amounts of CRV and Nis were chosen *i.e.*, 100% CRV, 75% CRV and 25% Nis, 50% CRV and 50% Nis, 25% CRV and 75% Nis, and 100% Nis, according to Table 1. The fourth column of Table 1 refers to the effective concentration of nisin in the PLA-based mats according to the concentration of bacteriocin in the Nis formulation used in this work (>2.5 wt%, as declared by the supplier). The additive concentrations were chosen according to scientific literature [44].

The PLA, and PLA/CRV/Nis mats were fabricated by adopting a semi-industrial electrospinning apparatus (NF-103, MECC Co., Ltd., Fukuoka, Japan). A 5 ml syringe equipped with a 19-gauge stainless steel needle was used as a polymeric solution reservoir. The solution flow rate was kept constant at 1 ml/h during the process. A cylindrical grounded rotary drum (diameter = 10 cm), positioned at a distance equal to 13 cm from the needle, was used as a collector. The other parameters used in the processing of PLA-based systems were the following: applied high voltage, 18 kV; temperature, 25 °C, collector angular speed, 10 rpm; processing time, 120 min. After processing, membranes with a thickness of around 70 μm were produced. In order to ensure the removal of any residual solvent, the collected materials were let dry under a fume hood for 48 h.

2.3. Morphological analysis

The morphology of the materials was assessed through scanning electron microscopy (Quanta 200 ESEM FEI, Hillsboro, OR, USA). Samples (circular shaped, diameter equal to 10 mm) were attached to an aluminum stub with conductive carbon tape. A Sputtering Scancoat Six (Edwards Laboratories, Milpitas, CA, USA) was used to sputter-coat the samples with gold for 60 s, in order to avoid electrostatic discharge during the test. The SEM was set with an accelerated voltage equal to 10 kV.

2.4. Particles size and fiber diameter distributions

A dedicated image processing software was used to investigate the fiber diameter and the particle size distribution of the electrospun mats. ImageJ on SEM images of AS and CLO particles was used to determine the particle size distribution, while a plugin for ImageJ (DiameterJ) was used to investigate the fiber diameter distribution [45].

2.5. Determination of encapsulation efficiency and loading capacity

The CRV and Nis encapsulation efficiency (*EE*) and loading capacity (*LC*) in PLA mats were assessed, agreeing to an experimental route described in our previous work [36]. Briefly, PLA/CRV/Nis electrospun samples (6 mg) were solubilized in chloroform (100 ml) for 12 hours. The real amount of CRV and Nis loaded in the mats was measured by means of an UV-Vis spectroscopy (Model UVPC 2401, Shimadzu Italia s.r.l., Milan, Italy). In particular, the wavelength at 273 nm for CAR and 222 nm for Nis were monitored and compared to a predetermined calibration curve of CRV/$CHCl_3$ and Nis/$CHCl_3$ solutions [43]. As references, PLA/$CHCl_3$ solution at 10 wt% of PLA was used. Each assay was carried out in triplicate. The encapsulation efficiency and loading capacity of the additives were calculated from Equations (1) and (2) respectively [43]:

$$EE\,[\%] = \frac{\text{Effective concentration of additive}}{\text{Theroretical concentration of additive}} \cdot 100 \quad (1)$$

$$LC\,[\%] = \frac{\text{Effective wight of additive}}{\text{Weight of PLA} - \text{based mats}} \cdot 100 \quad (2)$$

2.6. Mechanical properties

A universal testing machine (UTM, Instron, Norwood, MA, USA, model 3365) set with a 1 kN load cell was used to achieve the tensile mechanical measurements. The specimens (10×90 mm, thickness evaluated before each test) were cut off by the radial direction of the cylinder-shaped collector. The tensile tests were carried at 1 mm/min crosshead speed until the break. The working distance between the UTM jaws was 20 mm. The nominal stress-strain curves

were used to assess the elastic modulus (E), tensile strength (TS), and deformation at break (ε_b) of the samples. Seven samples were tested for each material, and the average values of the mechanical parameters were reported±their standard deviations.

2.7. Differential scanning calorimetry

The calorimetric properties of the samples were assessed via differential scanning calorimetry (DSC), (Setaram, model DSC131 evo, Lyon, France). The calorimeter was set to perform two heating cycles from 25 to 190 °C at 10 °C/min rate underneath nitrogen flow. The pre-weighted electrospun samples (~5 mg) were sealed in aluminum pans before testing. The crystallinity degree (χ) of electrospun PLA and PLA-based materials was calculated according to Equation (3) [46]:

$$\chi\,[\%] = \frac{\Delta H_m - \Delta H_{cc}}{\Delta H^0_{PLA} \cdot X_{PLA}} \cdot 100 \qquad (3)$$

where ΔH_{cc} is the cold crystallization enthalpy, and ΔH_m is the melting enthalpy of the samples, respectively. The weight fraction of PLA is X_{PLA}, while ΔH^0_{PLA} represents the melting enthalpy of 100% crystalline PLA (93.7 J/g) [46].

2.8. Water contact angle measurements

Static contact angles measurements were assessed via FTA 1000 (First Ten Ångstroms, Cambridge, UK) instrument. About 4 µl of distilled water was released on the samples. The images were acquired after 10 s from the deposition. At least 7 acquisitions were taken from each PLA-based material.

2.9. Carvacrol and nisin release kinetics

Before assessing the CRV and Nis release curves as a function of time, a calibration line was created correlating the UV-vis absorbance peak intensity and the CRV or Nis concentration [mg/l] in distilled water. In particular, CRV/water or Nis/water mixtures at different concentrations from 1 to 50 mg/l of CRV and from 50 to 1000 mg/l of Nis formulation were prepared and analyzed via UV-Vis (model Specord 252 spectrophotometer, Analytik Jena, Jena, Germany). The maximum of the absorbance peaks was identified at a wavelength equal to 273 nm for CAR and 222 nm for Nis [43]. The calibration curve of the Nis formulation was corrected by taking into account that the nominal Nis concentration in the formulation is 2.5 wt%, as declared by the supplier. The release curves of PLA/CRV/Nis mats were evaluated by dipping a pre-weighed sample (rectangles of 10 ×3 cm, weight ~ 13 mg) in 10 ml of distilled water, cooled at 4 °C, at different time points. Then the UV-Vis absorbance at 273 nm for CRV and 222 nm for Nis was measured and compared to the calibration line to obtain the concentration. The materials were immersed in 10 ml of fresh distilled water pre-cooled at 4 °C, subsequently each time point. The release curves exhibit the cumulative release of CRV or Nis calculated by serially adding the CRV or Nis amount released after each time point.

2.10. Antibacterial activity determination

In view of their food bio-preservation, the *in vitro* evaluation of the inhibitory activities of a given film against pathogenic bacteria is necessary [2, 47, 48]. The antimicrobial properties of electrospun materials activated with carvacrol and nisin, individually or in combination, were evaluated *in vitro* against *Escherichia coli*, *Listeria monocytogenes*, *Salmonella* Enteritidis, and *Staphylococcus aureus*. These species represent the four main pathogens responsible for food-borne diseases in humans. The four strains used as indicators (sensitive to the inhibitory substances) belonged to the American Type Culture Collection (ATCC). The cultures were grown in Brain Heart Infusion (BHI) broth (Oxoid, Milan, Italy) at 37 °C per 24 h and prepared for the inhibitory test by centrifugation at 10 000·g for 5 min to separate the cells from the supernatant, washing, and re-suspension in Ringer's solution (Sigma-Aldrich, Milan, Italy). The antimicrobial activity of the electrospun materials against the different strains was evaluated as reported by Llana-Ruiz-Cabello *et al*. [47] using a liquid medium to allow the release of the antibacterial substances. Briefly, 20 ml volume sterile cups (Biogenerica Srl, Pedara, Italy) containing 6 mL of sterile saline solution [NaCl 0.9% (w/v)] and 10 strips (1 cm×5 cm) of active or control electrospun materials were inoculated with the cell suspensions of each indicator strain at the final concentration of 10^6 CFU/ml and incubated at 37 °C until 3 d. Just after inoculation (0 d) and after 1 and 3 d of incubation, the cell suspensions were serially diluted by applying a dilution factor 1:10 in Ringer's solution (Sigma-Aldrich, Milan, Italy). The cell suspensions were inoculated on selective agar media to enumerate the four pathogenic bacteria, as reported in Table 2.

Table 2. Microorganisms and growth conditions.

Microorganisms	Media	Incubation conditions	Company
Escherichia (*E.*) *coli*	Chromogenic Medium	37 °C for 24 h	Condolab, Madrid, Spain
Listeria (*L.*) monocytogenes	*Listeria* Selective Agar Base	37 °C for 24 h	Oxoid, Milan, Italy
Salmonella (*S.*) Enteritidis	Hektoen Enteric Agar	37 °C for 24 h	Microbiol Diagnostici, Uta, Italy
Staphylococcus (*St.*) *aureus*	Baird Parker	37 °C for 48 h	Oxoid, Milan, Italy

Microbiological counts were carried out in duplicate.

3. Results and discussion

3.1. Morphology of the electrospun mats

Figure 1 shows the morphology of the Nis formulation used in this work. Nis was derived from milk, and the commercial powder used in this work contained milk proteins, carbohydrates, and sodium chloride. Indeed, it was possible to individuate spherical nisin particles dispersed together with the other components. The NaCl particles with lengths ranging from 5 up to 14 µm formed clusters from 10 to 60 µm.

The morphologies of the electrospun materials are displayed in Figure 2, together with their corresponding diameter size distribution. As expected and coherently with previous works [46, 49], the fibers are in the microscale and randomly oriented. More in detail, three main dimensions ranges can be distinguished: small nano-scaled fibers in the range 0.1–0.3 µm, medium fibers in the range 0.4–1.0 µm, and larger fibers in the range 1.0–1.7 µm. Interestingly, the relative frequency (*RF*) of each dimension range is dependent on the material composition. PLA displayed the highest *RF* for small and medium fibers, while the *RF* of the bigger fibers was relatively low. The addition of 20 wt% of CRV (PLA/CRV/Nis 20/0) caused a steep increase of the bigger fibers *RF* at the expense of small and medium fibers. As a result, the mean diameter size distribution increased from 0.63±0.36 µm of PLA to 1.00±0.40 µm of PLA/CRV/Nis 20/0, the highest among the systems here investigated. This result is coherent with other research articles focused on the preparation of PLA/CRV electrospun mat, and it was related to modifications in the solution viscosity in the presence of CRV [8, 16]. Altan *et al*. [50] highlighted an increase of apparent viscosity in PLA solution containing 20 wt% of CRV. Higher viscosity can lead to less stretching and reduced path of the jet, thus producing larger fibers. PLA/CRV/Nis 15/5 mats showed a morphology similar to PLA/CRV/Nis 20/0, although more small fibers were detected. Upon increasing the Nis content and concurrently reducing the CRV concentration, a gradual increase of the medium-range fibers was observed. In particular, the PLA/CRV/Nis 0/20 showed the highest *RF* in the medium-range fiber diameter and the lowest standard deviation of the fiber distribution. These results can be ascribed to the modifications induced by the additives on the solution properties. In fact, it is well known that the electrical conductivity of solutions can affect the shape and size of nanofibers [50]. Beachleya and Wen [51] observed that salt addition to PCL solutions increases its conductivity and the surface charge density of the solution jet, led to more homogenous electrospun fibers.

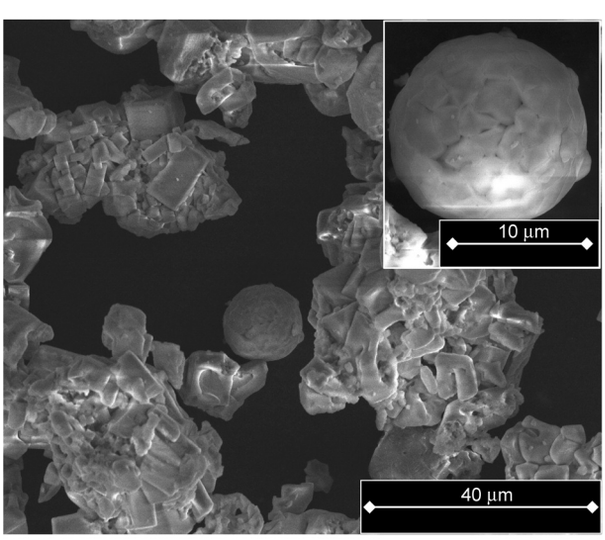

Figure 1. SEM images of the nisin formulation used in this work.

The additives also modified the fiber shape. More in detail, PLA, PLA/CRV/Nis 20/0, and PLA/CRV/Nis 15/5 showed smooth and regular fibers without drops or beads along the fibers. However, the high content of CRV in those systems caused a fiber flattening, particularly evident in the PLA/CRV/Nis 20/0 that were also characterized by a partial inter-fiber bonding. This result was already observed in similar systems [52, 53] and was ascribed to the plasticizer effect of the essential oil in the PLA matrix that will be discussed below.

Upon increasing the Nis content, and concurrently reducing the CRV concentration, a gradual decrease

in the fiber flattening and inter-fiber bonding can be observed. Moreover, PLA/CRV/Nis 10/10, 5/15, and 0/20 clearly display NaCl crystals embedded in the PLA fibers (see inset in Figure 2, PLA/CRV/Nis 0/20). As expected, the number of NaCl particles increased upon increasing the Nis concentration. The NaCl particles, well dispersed within the fibers, have a length ranging from 5 µm up to 10 µm, the same dimension as the NaCl particles forming the cluster observed in Figure 1. Reasonably, the solution was able to solubilize the other components on the Nis formulation, thus disgregating the NaCl clusters.

In terms of applicability of the PLA-based mats as antimicrobial material, the good dispersion of both the antimicrobial additives within the polymer matrix observed via SEM analysis can ensure a uniform release of the compounds when in contact with food. Furthermore, the high interconnected porous structure observed in all the systems potentially allows for moisture or exudates absorption when in contact with foods and/or vegetables.

3.2. Wettability of the electrospun mats

The modification induced by the additives on the hydrophilic/hydrophobic character of the materials was analyzed through water contact angle (*WCA*) measurements (Figure 3).

When considering porous materials for food packaging applications, adequate wettability is a desirable material property because it can ease the absorption

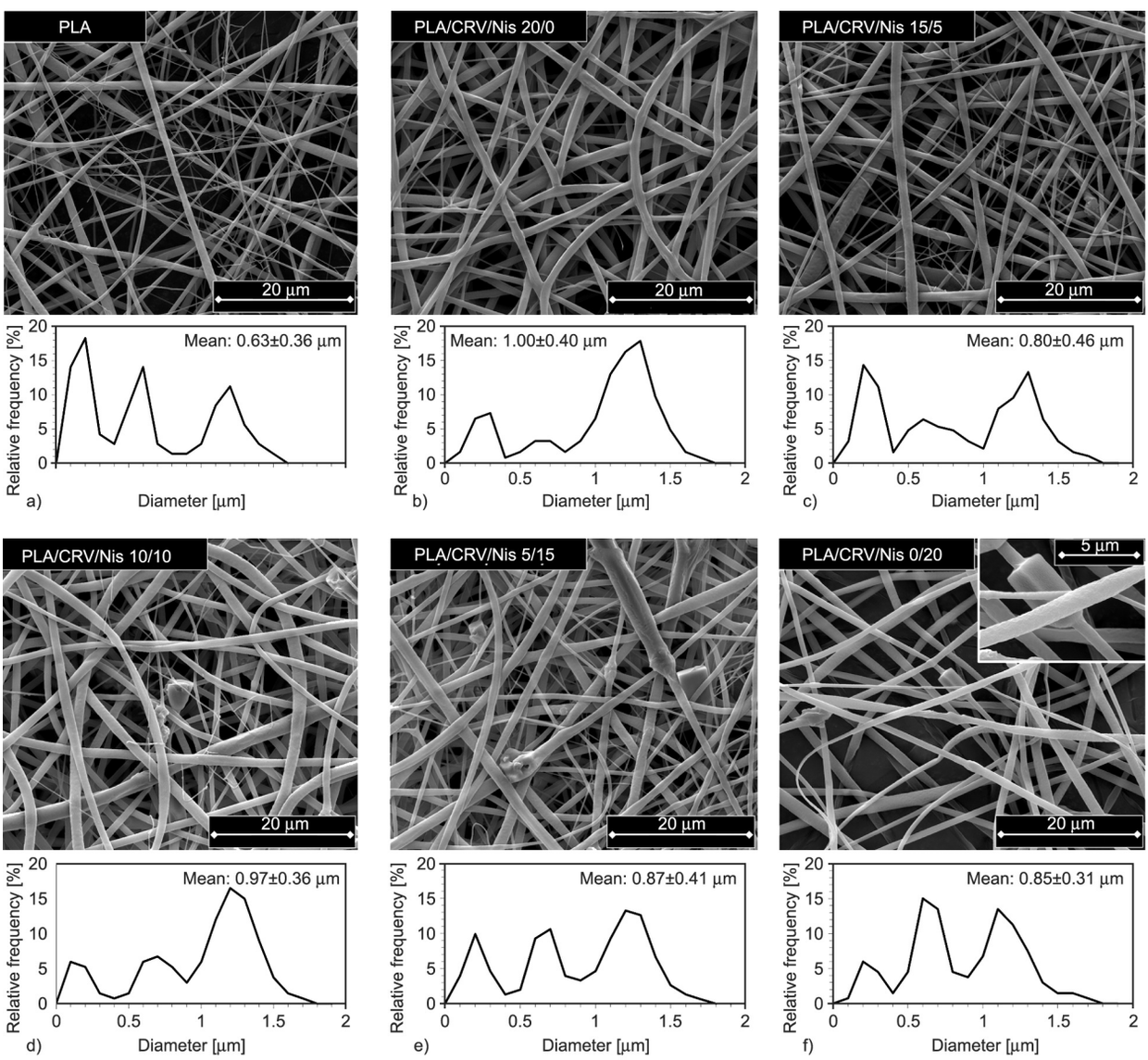

Figure 2. Scanning electron microscopy micrographs of PLA and PLA/CRV/Nis electrospun mats at different CRV/Nis relative concentrations and their corresponding fiber diameter distribution. a) PLA, b) PLA/CRV/Nis 20/0, c) PLA/CRV/Nis 15/5, d) PLA/CRV/Nis 10/10, e) PLA/CRV/Nis 5/15, f) PLA/CRV/Nis 0/20.

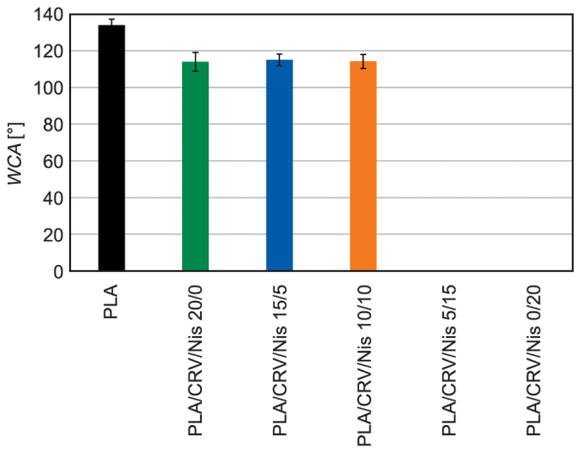

Figure 3. Water contact angles of PLA and PLA/CRV/Nis electrospun materials. Values are given as means ±SD.

of moisture or exudates produced by physicochemical modifications in foods and/or vegetable transpiration [54].

The intrinsic hydrophobicity of the electrospun PLA mats was highlighted by the high *WCA* values, around 133°. The addition of CRV (PLA/CRV/Nis 20/0) led to a reduction of the *WCA* of the samples from 130 down to 115°. This result was already observed in previous works, and it could be ascribed to the chemical structure of CRV that contains oxygenated moieties, which can interact with the water molecules [55]. Similar values of *WCA* were also recorded for the PLA/CRV/Nis 15/5 and 10/10 systems. The *WCA* values reached the value of 0° (water droplet rapidly absorbed by the porous material) for the system containing the highest amount of Nis *i.e.*, PLA/CRV/Nis 5/15 and 0/20. This result is not surprising since it was already observed in similar systems [56] and related to the presence of the non-fat dry milk compounds and the hygroscopic NaCl particles contained in the commercial nisin formulation that could provide the fast water absorption by the PLA/CRV/Nis 5/15 and 0/20 materials. For those systems, the presence of the NaCl particles probably led to capillary forces stronger than the water surface tension, thus allowing the absorption of the water droplet. According to these results, PLA/CRV/Nis 5/15 and 0/20 showed the highest potential as a collector of moisture or exudates produced by foods and/or vegetable transpiration.

3.3. Thermal and mechanical properties of electrospun mats

DSC analysis was implemented to evaluate the thermal transitions of the electrospun materials. The first-heating thermograms of the different PLA/CRV/Nis formulations are reported in Figure 4, while their main thermal properties are summarized in Table 3.

The thermogram of PLA was characterized by an endothermic peak at 62.8 °C, typically related to its glass transition (T_g). The same curve revealed a cold crystallization exothermic peak at 110.2 °C (T_{cc}) and a melting peak at 157.0 °C (T_m). More in detail, PLA presented a double melting peak characterized by a dominant peak at the highest temperature. These two melting peaks were already observed in scientific literature and related to the formation of two crystalline polymorphs: β crystalline form (at a lower temperature) and α crystalline form (at a higher temperature) [57].

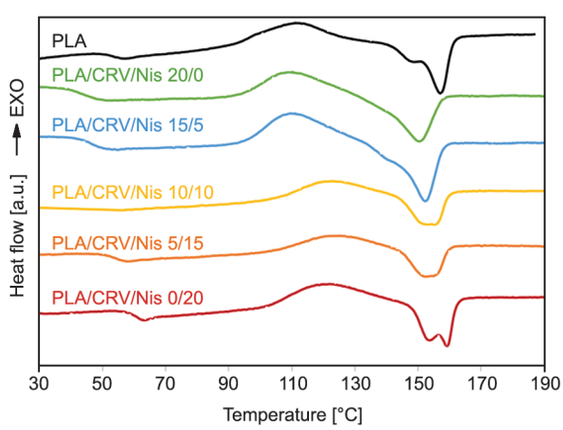

Figure 4. Differential scanning calorimetry (DSC) thermograms of electrospun PLA and PLA/CRV/Nis samples.

Table 3. DSC results of electrospun PLA and PLA/CRV/Nis samples.

Sample	T_g [°C]	T_{cc} [°C]	T_m [°C]	ΔH_{cc} [J/g]	ΔH_m [J/g]	χ [%]
PLA	62.8	110.2	157.0	22.30	30.1	8.32
PLA/CRV/Nis 20/0	48.1	109.5	150.5	24.49	27.51	4.02
PLA/CRV/Nis 15/5	51.1	110.1	152.3	27.10	31.87	4.66
PLA/CRV/Nis 10/10	52.1	120.3	152.6	13.41	16.45	4.06
PLA/CRV/Nis 5/15	57.5	120.3	155.5	13.92	16.9	3.98
PLA/CRV/Nis 0/20	62.9	120.0	159.1	18.50	24.7	8.27

PLA crystallinity was found to be relatively low, equal to 8.32%. This result was expected since electrospinning processing involves the rapid solidification of the polymeric solution due to solvent evaporation, thus avoiding the achievement of high crystallization degrees [58].

The inclusion of 20 wt% of CRV (PLA/CRV/Nis 20/0 system) caused a neat reduction of T_g and of T_m down to 48.1 and 150.5 °C, respectively. Interestingly, the melting peak is characterized by a unique peak at a lower temperature, thus indicating that PLA/CRV/Nis 20/0 exhibits one crystalline phase. Several researchers [59, 60] have observed similar melting behavior for PLA loaded with essential oils and can probably be ascribed to their molecular structure, likely able to modify the overall chain mobility of polymer matrix, resulting in a different crystallization phase. Moreover, the crystallinity of PLA was found to be more than halved by the addition of CRV (Table 4). These effects were already observed in previous works, and they were associated with the plasticizer action of CRV on PLA matrix [59, 60].

On the other hand, if compared to PLA, PLA/CRV/Nis 0/20 thermal properties were very similar since the only differences were observed for an increase of T_{cc} and a very slight increase of T_m. As a consequence, it may be assumed that the Nis formulation poorly affected the thermal properties of PLA, probably because of the low affinity existing among the polymer matrix and the main component of the formulation *i.e.*, NaCl particles.

The other formulation displayed T_g and T_m values in between PLA/CRV/Nis 20/0 and 0/20, which increased upon decreasing the CRV content (Table 3). T_{cc} values of PLA, PLA/CRV/Nis 20/0, and 15/5 were similar to each other and increased by about 10 °C for the other formulations. This result may be ascribed to the presence of NaCl particles that are able to reduce the PLA chain mobility, thus delaying the cold crystallization phenomenon.

The shape of the melting peak of PLA/CRV/Nis 15/5 was very similar to that of PLA/CRV/Nis 20/0, while the onset of the second melting peak observed in PLA is evident in the other materials. Interestingly the height of the higher-temperature melting peak increased upon increasing the content of Nis, although the lower-temperature peak in PLA/CRV/Nis 0/20 is more pronounced than in PLA.

The values of crystallinity for all the systems containing carvacrol were in the range 4–4.7 %, thus corroborating the hypothesis that the driver component able to reduce this value is CRV, also at low concentration.

The mechanical properties of the materials were evaluated through tensile tests. Figure 5 displays the engineering stress-strain curves of the electrospun mats, while Table 4 summarizes the mean mechanical parameters. PLA exhibited the mechanical comportment of a ductile material displaying relatively low *E*, around 19 MPa, and relatively high elongation at break (ε_b), around 140%. The addition of 20 wt% of CRV (PLA/CRV/Nis 20/0) led to an increase of both elastic modulus, up to 112 MPa, and ε_b up to 190%. An increase of the tensile strength from 3.3 MPa of PLA to 4.7 MPa of PLA/CRV/Nis 20/0 was also recorded.

PLA/CRV/Nis 15/5 presented *E* values higher than PLA (105.6 MPa) and lower values of *TS* and ε_b equal to 4.7 MPa and 129%, respectively. Upon increasing the Nis content and concurrently reducing the CRV concentration, a gradual decrease of all the

Table 4. Tensile properties of electrospun PLA and PLA/CRV/Nis samples. Values are given as means ±SD of n = 5 samples.

Sample	*E* [MPa]	*TS* [MPa]	ε [%]
PLA	19.1±2.1	3.3±0.5	142.1±15.4
PLA/CRV/Nis 20/0	111.9±9.3	4.7±0.3	189.7±13.3
PLA/CRV/Nis 15/5	105.6±8.0	2.3±0.7	128.9±17.5
PLA/CRV/Nis 10/10	88.9±8.8	2.1±0.4	109.8±9.7
PLA/CRV/Nis 5/15	53.8±3.7	0.7±0.1	16.6±2.5
PLA/CRV/Nis 0/20	37.0±3.1	0.7±0.1	7.7±1.2

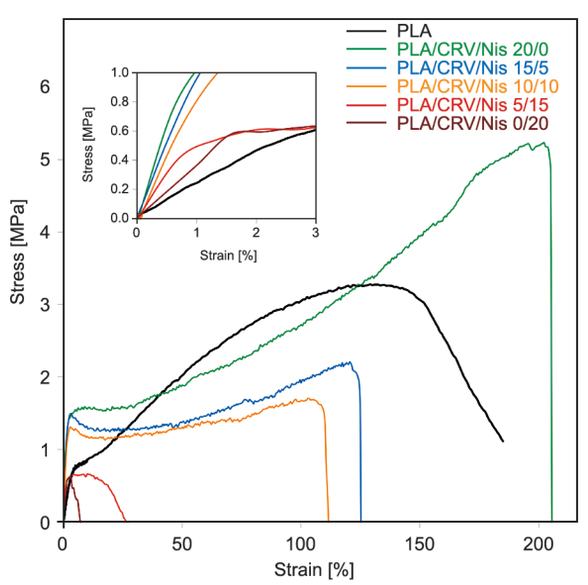

Figure 5. Representative stress-strain curves of electrospun PLA and PLA/CRV/Nis samples.

mechanical parameters can be observed. In particular, the electrospun material loaded with 20 wt% of Nis (PLA/CRV/Nis 0/20) showed an elastic modulus higher than PLA (37 MPa) and the lowest values of *TS* and ε_b among the materials investigated, equal to 0.7 MPa and 7.7%, respectively.

The steep increase of all the mechanical parameters due to the presence of CRV was already observed in previous work [60] and related to a double action of CRV that acted as a plasticizer and as adhesive for the PLA fibers. The plasticizer action of this essential oil on a biodegradable polymer matrix was previously reported [59, 60] and ascribed to the capacity of the low molecular weight CRV molecules to reduce the intermolecular forces of the polymer chains. As a result, CRV is able to increase the elongation at break of the matrix. Moreover, CRV can enhance the surface interactions of the PLA-based fibers, hindering their slipping results in an increase in the elastic modulus of the membranes [8, 60].

The value of the elastic modulus of PLA/CRV/Nis 0/20, almost double that of PLA, let us reasonably conclude that the Nis formulation has a certain reinforcing action on PLA. This is not surprising since the addition of solid particles usually leads to an increase in the elastic modulus of electrospun polymer matrices [46, 61]. However, the same materials displayed a dramatic reduction of the elongation at break, which allowed identifying the NaCl particles embedded into the PLA fibers as defects, as already observed in other works focused on nisin inclusion in gelatin electrospun fibers [61] and PLA/hydroxyapatite electrospun composites [46].

In fact, solid particles embedded in electrospun fibers can act as confined stress points that are able to induce the fracture of the material at lower strain [46]. The premature failure of the samples may be identified as the reason for the low *TS* values observed for those samples [46].

As expected, PLA/CRV/Nis 15/5, 10/10, and 5/15 showed an intermediate mechanical behavior between PLA/CRV/Nis 20/0 and 0/20. Since PLA/CRV/Nis 15/5 deformation at break is slightly lower than that of PLA, it can be assumed that the Nis formulation is likely able to moderate the plasticizer effect of CRV also at low concentrations.

Due to the relatively high elastic modulus and elongation at break displayed by PLA/CRV/Nis 20/0, 15/5, and 10/10, these materials can be adapted for use as high load-bearing packaging materials. On the other hand, PLA/CRV/Nis 5/15 and 0/20 are more suitable for low deformation applications, such as direct food wrapping, because of their fragile mechanical behavior.

3.4. Encapsulation efficiency and release kinetic of CRV and Nis

Encapsulation efficiency (*EE*) and loading capacity (*LC*) represent key parameters for assessing the achievability of antibacterial electrospun materials. *EE* can be defined as the percentage of additive that becomes encapsulated during the processing [62]. The higher the *EE*, the lower the additive loss due to the fabrication route. On the other hand, the loading capacity can be defined as the concentration of additive that the carrier is able to entrap. The higher the *LC*, the higher the additive concentration that the material can potentially release.

The *EE* and *LC* of CRV and Nis incapsulated in PLA/CRV/Nis electrospun mats are summarized in Table 5. CRV showed *EE* values that increased upon decreasing the CRV concentration in the polymer matrix. On the opposite, Nis *EE* values slightly increased upon increasing the Nis concentration, and they were always higher than that of CRV. This result can be ascribed to the different *EE* loss mechanisms among the two systems. In fact, it is reasonable to suppose that part of CRV was not encapsulated into the PLA fibers due to its high volatility, which caused partial evaporation during the jet spinning [63]. Therefore, the higher the CRV concentration, the higher the evaporation driving force and the lower the *EE* of this component. On the other side, Nis *EE* can be mainly ascribed to the sedimentation of the Nis particles during the electrospinning process. More in detail, the equipment used in this work exploits a horizontal syringe pump that permits the deposition of part of the Nis formulation on its bottom during processing.

Table 5. CRV and Nis encapsulation efficiency and loading capacity in electrospun PLA/CRV/Nis samples.

Sample	Encapsulation efficiency [%]		Loading capacity [%]	
	CRV	Nis	CRV	Nis
PLA/CRV/Nis 20/0	85.6	–	17.12	–
PLA/CRV/Nis 15/5	87.4	91.7	13.11	4.585
PLA/CRV/Nis 10/10	89.7	92.4	8.97	9.24
PLA/CRV/Nis 5/15	92.3	93.1	4.615	13.965
PLA/CRV/Nis 0/20	–	94.7	–	18.94

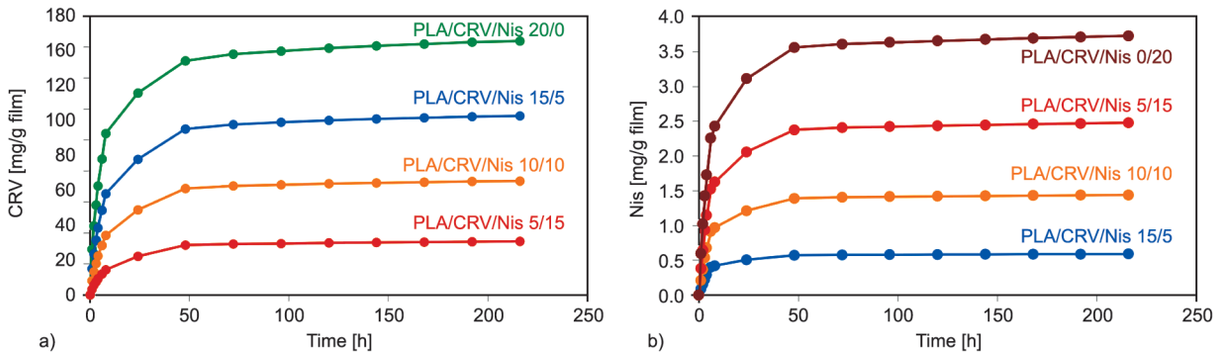

Figure 6. Release kinetics of a) CRV and b) Nis from PLA/CRV/Nis samples in distilled water at 4 °C expressed as mg of released additive for 1 g of electrospun mat *versus* time.

However, due to the high dispersion achieved during mixing, the Nis *EE* was relatively high and slightly dependent on the Nis concentration. For both additives, the *EE* values found in this work are high (> 80% [64]) and comparable to those found in other similar systems [65–67].

PLA electrospun mats displayed an increase in the LC of both the antimicrobial additive used upon increasing their concentration, in agreement with scientific literature [62]. The high values of loading capacity are in agreement with other results in scientific literature and confirm that the electrospinning process is very efficient for the encapsulation of active compounds in nanostructured materials [63, 68].

The release profile of CRV and Nis from the different PLA/CRV/Nis formulations are displayed in Figures 6a and 6b, respectively, as the mg of additive released for 1 mg of material.

The curves indicate that the amount of released additive is proportional to its concentration in the PLA-based material. In general, the value of Nis released from 1 gram of membrane is much lower than that of CRV since the commercial formulation used in this work contains 2.5 wt% of Nis.

One of the most adopted models to analyze the release mechanism of additives embedded in electrospun systems is the power-law model. For this reason, Figure 7 reports the experimental data plotted as log (M_t/M_∞) *versus* log (time) fitted by a power law (Equation (4)):

$$\frac{M_t}{M_\infty} = kt^n \tag{4}$$

where M_∞ represents the weight of CRV or Nis incorporated in the polymer matrix, according to the encapsulation efficiency results; M_t stays for the quantity of CRV or Nis released at time t; k is a kinetics constant; t is the release time; n is the diffusion exponent according to Peppas and Sinclair [69].

Table 6 summarizes n, k, and R^2 obtained by fitting the experimental data with the power law. According to our previous works, the power-law model was used to fit separately three release stages that can be distinguished by the linearity of the log (M_t/M_∞) *versus* log (time) curves [8]. According to this approach, both the CRV and Nis release were characterized by three different release stages *i.e.*, a burst stage (I) before 8 and 6 hours of release for CRV and Nis, respectively; a

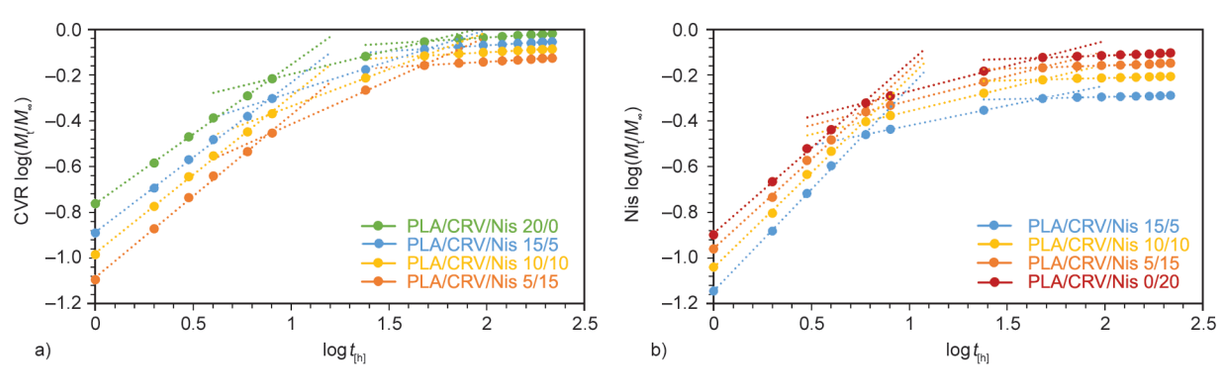

Figure 7. Release kinetics of a) CRV and b) Nis from PLA/CRV/Nis samples in distilled water at 4 °C expressed as log (M_t/M_∞) *versus* log (time).

Table 6. Power law parameters were obtained from the release kinetics of Nis and CRV from PLA/CRV/Nis samples.

CRV release	Release stage	k [h^{-1}]		$n \cdot 10^{-2}$ [–]		R^2 [–]	
		CRV	Nis	CRV	Nis	CRV	Nis
PLA/CRV/Nis 20/0	(I)	–0.76	–	60.9	–	99.9	–
	(II)	–0.40	–	20.7	–	100.0	–
	(III)	–0.14	–	5.3	–	99.4	–
PLA/CRV/Nis 15/5	(I)	–0.89	–1.14	65.5	89.0	99.9	99.9
	(II)	–0.55	–0.60	27.5	17.5	99.9	100.0
	(III)	–0.17	–0.33	4.9	1.9	99.4	99.2
PLA/CRV/Nis 10/10	(I)	–0.98	–1.04	68.6	83.1	99.9	99.8
	(II)	–0.66	–0.56	32.4	20.3	100.0	100.0
	(III)	–0.19	–0.26	4.6	2.2	99.4	99.4
PLA/CRV/Nis 5/15	(I)	–1.09	–0.96	71.2	78.2	99.8	99.8
	(II)	–0.80	–0.53	38.2	21.4	99.9	100.0
	(III)	–0.24	–0.21	4.7	2.7	99.8	99.6
PLA/CRV/Nis 0/20	(I)	–	–0.89	–	74.7	–	99.8
	(II)	–	–0.49	–	22.0	–	99.8
	(III)	–	–0.17	–	3.0	–	99.6

slower release rate (II) (for 8–48 hours and 6–48 hours of release for CRV and Nis, respectively); a final plateau region (III) from 48 hours up to the end of the test for both the additives, indicating a slow and sustained release up to 216 hours.

During the first release stage, both CRV and Nis release is characterized by n values higher than 0.5, thus suggesting a superposition of diffusion-controlled and swelling-controlled release defined as anomalous transport according to Peppas and Sinclair [69]. During the second and third release stage, the diffusion exponent values for CRV and Nis were lower than 0.5, suggesting a diffusion-controlled release, according to Peppas and Sinclair [69].

More in detail, during the first release stage, n values of Nis are higher than those of CRV, while during the second and third stages, the diffusion exponent of Nis showed a steep decrease leading to lower n values than those of the CRV. This result suggested a more intense Nis burst release than that of CRV during the first hours of the test.

According to these results, it can be concluded that the materials proposed in this work as suitable for fresh products characterized by a relatively short shelf-life.

3.5. Antibacterial activity of electrospun mats

In this study, the inhibitory activity of the electrospun mats activated with CRV and Nis, alone or in combination, was tested against different bacteria generally used as food safety criteria (*L. monocytogenes* ATCC19114 and *S.* Enteritidis ATCC13076) and process hygiene criteria (*E. coli* ATCC25922 and *St. aureus* ATCC33862) following the indication of European Commission (EC) Regulation No 2073/2005 (Commission Regulation, 2005). As reported in Table 6, just after bacterial inoculation, all samples showed a cell density of approximately 6.0 log CFU/ml. A decrease in microbial growth was registered for all strains in the presence of PLA activated with 20% CRV. The decrease in level was significant for all four pathogens from the first day, and *E. coli* and *St. aureus* were undetectable on the third day. These observations are not surprising because CRV was found to exert inhibition of food-borne pathogenic bacteria in several polymeric matrices [16, 36, 43]. CRV reduces the growth of Gram-negative bacteria thanks to its ability to destroy their double-layer cell membrane [70]. On the other hand, PLA/ CRV/Nis 0/20 showed a lower antimicrobial activity against all the food-borne bacterial pathogens tested in this work. This result can be explained by considering the low absolute amount of Nis released by the polymer matrix because the commercial formulation used in this work contains 2.5 wt% of nisin. As summarized in Table 7, the antimicrobial activity of the electrospun materials activated with both CRV and Nis decreased with the percentage of Nis added, confirming the previous findings of Lopresti *et al*. [43]. This result corroborates the hypothesis that in the ternary PLA/CRV/Nis systems, the antimicrobial action can

Table 7. Antimicrobial activity of electrospun PLA and PLA/CRV/Nis samples against the main food-borne bacterial pathogens.

Strains/Samples	Antimicrobial activity [log CFU/ml]		
	Day 0	Day 1	Day 3
***E. coli* ATCC25922**			
PLA	6.07±0.10	6.06±0.09	6.04±0.06
PLA/CRV/NIS 20/0	6.04±0.06	1.68±0.02	0.00±0.00
PLA/CRV/NIS 15/5	6.01±0.15	4.15±0.21	3.58±0.03
PLA/CRV/NIS 10/10	5.99±0.06	4.80±0.28	4.68±0.02
PLA/CRV/NIS 5/15	5.90±0.14	5.25±0.07	5.05±0.07
PLA/CRV/NIS 0/20	5.91±0.16	5.49±0.02	5.26±0.08
***L. monocytogenes* ATCC19114**			
PLA	6.12±0.16	6.05±0.07	6.05±0.07
PLA/CRV/NIS 20/0	5.90±0.14	3.16±0.02	1.53±0.04
PLA/CRV/NIS 15/5	6.02±0.03	4.05±0.07	3.70±0.14
PLA/CRV/NIS 10/10	6.09±0.12	5.32±0.02	4.19±0.02
PLA/CRV/NIS 5/15	6.10±0.28	5.34±0.06	5.24±0.06
PLA/CRV/NIS 0/20	6.04±0.06	5.66±0.06	5.53±0.05
***S.* Enteritidis ATCC13076**			
PLA	6.02±0.03	5.95±0.07	5.95±0.07
PLA/CRV/NIS 20/0	6.06±0.08	3.15±0.03	1.54±0.06
PLA/CRV/NIS 15/5	6.06±0.08	4.46±0.02	3.68±0.02
PLA/CRV/NIS 10/10	6.05±0.07	5.16±0.03	4.77±0.01
PLA/CRV/NIS 5/15	5.99±0.02	5.35±0.07	5.06±0.08
PLA/CRV/NIS 0/20	5.91±0.16	5.49±0.12	5.15±0.21
***St. aureus* ATCC33862**			
PLA	6.02±0.03	5.97±0.23	5.95±0.21
PLA/CRV/NIS 20/0	6.05±0.22	2.35±0.07	0.00±0.00
PLA/CRV/NIS 15/5	6.05±0.07	4.67±0.10	3.56±0.03
PLA/CRV/NIS 10/10	6.12±0.17	4.91±0.13	4.15±0.03
PLA/CRV/NIS 5/15	6.07±0.09	5.20±0.01	5.04±0.06
PLA/CRV/NIS 0/20	6.09±0.12	5.65±0.07	5.40±0.14

Abbreviations: *E.* – *Escherichia*; *L.* – *Listeria*; *S.* – *Salmonella*; *St.* – *Staphylococcus*.

be mainly ascribed to the release of CRV rather than to Nis.

5. Conclusions

This work focused on the chemo-physical characterization and antimicrobial potential of PLA-based electrospun membranes loaded with different relative amounts CRV and Nis, two well-known antimicrobial agents, commercially available and GRAS food additives by the U.S. FDA.

The SEM images revealed that the CRV/Nis relative concentrations affected the diameter size distributions of the PLA fibers. A higher concentration of CRV led to a higher mean diameter size that became smaller upon increasing the Nis content. High Nis concentration also switched the wettability behavior of the samples from hydrophobic to hydrophilic. Thermal and tensile tests assessed the plasticizer action of CRV on PLA, while the Nis formulation was found to modify the mechanical behavior of the membranes from ductile to brittle without modifying its thermal behavior. Moreover, CRV and Nis formulations were able to improve the elastic modulus of the PLA-based membranes by acting in different ways. CRV avoided the fiber slipping during the tensile test and induced an elastic improvement of about 580% for the PLA/CRV/Nis 20/0 systems, while the Nis formulation acted as a solid filler incrementing the elastic modulus of the PLA/CRV/Nis 0/20 membranes of about 100%. The other materials showed intermediate values of the elastic modulus. The release curves analyses revealed the amount of released additive is proportional to its concentration in the PLA-based material. The power-law model allowed

assessing that the burst release of CRV was slower than that of Nis in all the investigated formulations, although both the additives were characterized by an anomalous-transport mechanism of release. The electrospun material containing 20% of CRV exhibited the highest inhibitory activity against *E. coli*, *L. monocytogenes*, *S.* Enteritidis, and *St. aureus*.

Acknowledgements

Funding: Francesco Lopresti is funded by the European Social Fund (ESF) – PON A.I.M: Attraction and International Mobility_ AIM1845825 – 1. CUP: B74I18000260001.
The authors want to thank the 'Biomaterials analysis and preparation' laboratory of the ATeN Center for the electrospinning equipment.

References

[1] Mangaraj S., Yadav A., Bal L. M., Dash S. K., Mahanti N. K.: Application of biodegradable polymers in food packaging industry: A comprehensive review. Journal of Packaging Technology and Research, **3**, 77–96 (2019). https://doi.org/10.1007/s41783-018-0049-y

[2] Lopresti F., Botta L., Scaffaro R., Bilello V., Settanni L., Gaglio R.: Antibacterial biopolymeric foams: Structure–property relationship and carvacrol release kinetics. European Polymer Journal, **121**, 109298 (2019). https://doi.org/10.1016/j.eurpolymj.2019.109298

[3] Xu W., Wang X., Sandler N., Willför S., Xu C.: Three-dimensional printing of wood-derived biopolymers: A review focused on biomedical applications. ACS Sustainable Chemistry and Engineering, **6**, 5663–5680 (2018). https://doi.org/10.1021/acssuschemeng.7b03924

[4] Mostofizadeh M., Ghasemi-Mobarakeh L., Zamani M.: Dual drug release from gelatin/PLGA core–shell fibers for diabetic neuropathic wound healing. Macromolecular Materials and Engineering, **307**, 2100490 (2022). https://doi.org/10.1002/mame.202100490

[5] Czél Gy., Vanyorek L., Sycheva A., Kerekes F., Szőri-Dorogházi E., Janovszky D.: Antimicrobial effect of silver nanoparticles plated natural zeolite in polyurethane foam. Express Polymer Letters, **15**, 853–864 (2021). https://doi.org/10.3144/expresspolymlett.2021.68

[6] Torres-Martinez E. J., Bravo J. M. C., Medina A. S., González G. L. P., Gómez L. J. V.: A summary of electrospun nanofibers as drug delivery system: Drugs loaded and biopolymers used as matrices. Current Drug Delivery, **15**, 1360–1374 (2018). https://doi.org/10.2174/1567201815666180723114326

[7] Wu J., Zhang Z., Gu J., Zhou W., Liang X., Zhou G., Han C. C., Xu S., Liu Y.: Mechanism of a long-term controlled drug release system based on simple blended electrospun fibers. Journal of Controlled Release, **320**, 337–346 (2020). https://doi.org/10.1016/j.jconrel.2020.01.020

[8] Scaffaro R., Gulino F. E., Lopresti F.: Structure–property relationship and controlled drug release from multiphasic electrospun carvacrol-embedded polylactic acid/polyethylene glycol and polylactic acid/polyethylene oxide nanofiber mats. Journal of Industrial Textiles, **49**, 943–966 (2020). https://doi.org/10.1177/1528083718801359

[9] Ruiz-Ruiz F., Mancera-Andrade E. I., Parra-Saldivar R., Keshavarz T., Iqbal H.: Drug delivery and cosmeceutical applications of poly-lactic acid based novel constructs – A review. Current Drug Metabolism, **18**, 914–925 (2017). https://doi.org/10.2174/1389200218666170919170335

[10] Scaffaro R., Lopresti F., Marino A., Nostro A.: Antimicrobial additives for poly(lactic acid) materials and their applications: Current state and perspectives. Applied Microbiology and Biotechnology, **102**, 7739–7756 (2018). https://doi.org/10.1007/s00253-018-9220-1

[11] Herrero-Herrero M., Gómez-Tejedor J. A., Vallés-Lluch A.: PLA/PCL electrospun membranes of tailored fibres diameter as drug delivery systems. European Polymer Journal, **99**, 445–455 (2018). https://doi.org/10.1016/j.eurpolymj.2017.12.045

[12] Malek N. S. A., Faizuwan M., Khusaimi Z., Bonnia N. N., Rusop M., Asli N. A.: Preparation and characterization of biodegradable polylactic acid (PLA) film for food packaging application: A review. Journal of Physics: Conference Series, **1892**, 012037 (2021). https://doi.org/10.1088/1742-6596/1892/1/012037

[13] Alves P. E., Soares B. G., Lins L. C., Livi S., Santos E. P.: Controlled delivery of dexamethasone and betamethasone from PLA electrospun fibers: A comparative study. European Polymer Journal, **117**, 1–9 (2019). https://doi.org/10.1016/j.eurpolymj.2019.05.001

[14] Yang F., Wang J., Li X., Jia Z., Wang Q., Yu D., Li J., Niu X.: Electrospinning of a sandwich-structured membrane with sustained release capability and long-term anti-inflammatory effects for dental pulp regeneration. Bio-Design and Manufacturing, **5**, 305–317 (2021). https://doi.org/10.1007/s42242-021-00152-5

[15] Radusin T., Torres-Giner S., Stupar A., Ristic I., Miletic A., Novakovic A., Lagaron J. M.: Preparation, characterization and antimicrobial properties of electrospun polylactide films containing *Allium ursinum* L. extract. Food Packaging and Shelf Life, **21**, 100357 (2019). https://doi.org/10.1016/j.fpsl.2019.100357

[16] Scaffaro R., Lopresti F., D'Arrigo M., Marino A., Nostro A.: Efficacy of poly(lactic acid)/carvacrol electrospun membranes against *Staphylococcus aureus* and *Candida albicans* in single and mixed cultures. Applied Microbiology and Biotechnology, **102**, 4171–4181 (2018). https://doi.org/10.1007/s00253-018-8879-7

[17] Han C., Cai N., Chan V., Liu M., Feng X., Yu F.: Enhanced drug delivery, mechanical properties and antimicrobial activities in poly(lactic acid) nanofiber with mesoporous Fe_3O_4-COOH nanoparticles. Colloids and Surfaces A: Physicochemical and Engineering Aspects, **559**, 104–114 (2018).
https://doi.org/10.1016/j.colsurfa.2018.09.012

[18] Vidal C. P., Velásquez E., Galotto M. J., de Dicastillo C. L.: Antimicrobial food packaging system based on ethyl lauroyl arginate-loaded core/shell electrospun structures by using hydrophilic and hydrophobic polymers. Polymer Testing, **93**, 106937 (2021).
https://doi.org/10.1016/j.polymertesting.2020.106937

[19] Hajikhani M., Emam-Djomeh Z., Askari G.: Fabrication and characterization of mucoadhesive bioplastic patch *via* coaxial polylactic acid (PLA) based electrospun nanofibers with antimicrobial and wound healing application. International Journal of Biological Macromolecules, **172**, 143–153 (2021).
https://doi.org/10.1016/j.ijbiomac.2021.01.051

[20] Yuan Y., Choi K., Choi S-O., Kim J.: Early stage release control of an anticancer drug by drug-polymer miscibility in a hydrophobic fiber-based drug delivery system. RSC Advances, **8**, 19791–19803 (2018).
https://doi.org/10.1039/c8ra01467a

[21] Poláková L., Širc J., Hobzová R., Cocârță A-I., Heřmánková E.: Electrospun nanofibers for local anticancer therapy: Review of *in vivo* activity. International Journal of Pharmaceutics, **558**, 268–283 (2019).
https://doi.org/10.1016/j.ijpharm.2018.12.059

[22] Abid S., Hussain T., Raza Z. A., Nazir A.: Current applications of electrospun polymeric nanofibers in cancer therapy. Materials Science and Engineering: C, **97**, 966–977 (2019).
https://doi.org/10.1016/j.msec.2018.12.105

[23] Anup N., Chavan T., Chavan S., Polaka S., Kalyane D., Abed S. N., Venugopala K. N., Kalia K., Tekade R. K.: Reinforced electrospun nanofiber composites for drug delivery applications. Journal of Biomedical Materials Research Part A, **109**, 2036–2064 (2021).
https://doi.org/10.1002/jbm.a.37187

[24] Bakola V., Karagkiozaki V., Tsiapla A. R., Pappa F., Moutsios I., Pavlidou E., Logothetidis S.: Dipyridamole-loaded biodegradable PLA nanoplatforms as coatings for cardiovascular stents. Nanotechnology, **29**, 275101 (2018).
https://doi.org/10.1088/1361-6528/aabc69

[25] Zare M., Dziemidowicz K., Williams G. R., Ramakrishna S.: Encapsulation of pharmaceutical and nutraceutical active ingredients using electrospinning processes. Nanomaterials, **11**, 1968 (2021).
https://doi.org/10.3390/nano11081968

[26] Mohammadi M. A., Hosseini S. M., Yousefi M.: Application of electrospinning technique in development of intelligent food packaging: A short review of recent trends. Food Science and Nutrition, **8**, 4656–4665 (2020).
https://doi.org/10.1002/fsn3.1781

[27] Sameen D. E., Ahmed S., Lu R., Li R., Dai J., Qin W., Zhang Q., Li S., Liu Y.: Electrospun nanofibers food packaging: Trends and applications in food systems. Critical Reviews in Food Science and Nutrition, in press (2022).
https://doi.org/10.1080/10408398.2021.1899128

[28] Zhan F., Yan X., Sheng F., Li B.: Facile *in situ* synthesis of silver nanoparticles on tannic acid/zein electrospun membranes and their antibacterial, catalytic and antioxidant activities. Food Chemistry, **330**, 127172 (2020).
https://doi.org/10.1016/j.foodchem.2020.127172

[29] Zhang R., Lan W., Ji T., Sameen D. E., Ahmed S., Qin W., Liu Y.: Development of polylactic acid/ZnO composite membranes prepared by ultrasonication and electrospinning for food packaging. LWT, **135**, 110072 (2021).
https://doi.org/10.1016/j.lwt.2020.110072

[30] Fonseca L. M., dos Santos Cruxen C. E., Bruni G. P., Fiorentini Â. M., da Rosa Zavareze E., Lim L-T., Dias A. R. G.: Development of antimicrobial and antioxidant electrospun soluble potato starch nanofibers loaded with carvacrol. International Journal of Biological Macromolecules, **139**, 1182–1190 (2019).
https://doi.org/10.1016/j.ijbiomac.2019.08.096

[31] Lin L., Mao X., Sun Y., Rajivgandhi G., Cui H.: Antibacterial properties of nanofibers containing chrysanthemum essential oil and their application as beef packaging. International Journal of Food Microbiology, **292**, 21–30 (2019).
https://doi.org/10.1016/j.ijfoodmicro.2018.12.007

[32] Li T-T., Wang Y., Peng H-K., Zhang X., Shiu B-C., Lin J-H., Lou C-W.: Lightweight, flexible and superhydrophobic composite nanofiber films inspired by nacre for highly electromagnetic interference shielding. Composites Part A: Applied Science and Manufacturing, **128**, 105685 (2020).
https://doi.org/10.1016/j.compositesa.2019.105685

[33] Eom S., Park S. M., Han S. J., Kim J. W., Kim D. S.: One-step fabrication of a tunable nanofibrous well insert *via* electrolyte-assisted electrospinning. RSC Advances, **7**, 38300–38306 (2017).
https://doi.org/10.1039/c7ra06629e

[34] Scaffaro R., Maio A., D'Arrigo M., Lopresti F., Marino A., Bruno M., Nostro A.: Flexible mats as promising antimicrobial systems *via* integration of *Thymus capitatus* (L.) essential oil into PLA. Future Microbiology, **15**, 1379–1392 (2020).
https://doi.org/10.2217/fmb-2019-0291

[35] Biddeci G., Cavallaro G., Di Blasi F., Lazzara G., Massaro M., Milioto S., Parisi F., Riela S., Spinelli G.: Halloysite nanotubes loaded with peppermint essential oil as filler for functional biopolymer film. Carbohydrate Polymers, **152**, 548–557 (2016).
https://doi.org/10.1016/j.carbpol.2016.07.041

[36] Gaglio R., Botta L., Garofalo G., Miceli A., Settanni L., Lopresti F.: Carvacrol activated biopolymeric foam: An effective packaging system to control the development of spoilage and pathogenic bacteria on sliced pumpkin and melon. Food Packaging and Shelf Life, **28**, 100633 (2021). https://doi.org/10.1016/j.fpsl.2021.100633

[37] Guarda A., Rubilar J. F., Miltz J., Galotto M. J.: The antimicrobial activity of microencapsulated thymol and carvacrol. International Journal of Food Microbiology, **146**, 144–150 (2011). https://doi.org/10.1016/j.ijfoodmicro.2011.02.011

[38] Campos-Requena V. H., Rivas B. L., Pérez M. A., Figueroa C. R., Sanfuentes E. A.: The synergistic antimicrobial effect of carvacrol and thymol in clay/polymer nanocomposite films over strawberry gray mold. LWT-Food Science and Technology, **64**, 390–396 (2015). https://doi.org/10.1016/j.lwt.2015.06.006

[39] de Souza A. G., dos Santos N. M. A., da Silva Torin R. F., dos Santos Rosa D.: Synergic antimicrobial properties of Carvacrol essential oil and montmorillonite in biodegradable starch films. International Journal of Biological Macromolecules, **164**, 1737–1747 (2020). https://doi.org/10.1016/j.ijbiomac.2020.07.226

[40] Turgis M., Vu K. D., Dupont C., Lacroix M.: Combined antimicrobial effect of essential oils and bacteriocins against foodborne pathogens and food spoilage bacteria. Food Research International, **48**, 696–702 (2012). https://doi.org/10.1016/j.foodres.2012.06.016

[41] Churklam W., Chaturongakul S., Ngamwongsatit B., Aunpad R.: The mechanisms of action of carvacrol and its synergism with nisin against *Listeria monocytogenes* on sliced bologna sausage. Food Control, **108**, 106864 (2020). https://doi.org/10.1016/j.foodcont.2019.106864

[42] Food Drug Administration: Nisin preparation: Affirmation of GRAS status as a direct human food ingredient. Federal Register, **53**, 11247–11251 (1988).

[43] Lopresti F., Botta L., la Carrubba V., di Pasquale L., Settanni L., Gaglio R.: Combining carvacrol and nisin in biodegradable films for antibacterial packaging applications. International Journal of Biological Macromolecules, **193**, 117–126 (2021). https://doi.org/10.1016/j.ijbiomac.2021.10.118

[44] Koosha M., Mirzadeh H., Shokrgozar M. A., Farokhi M.: Nanoclay-reinforced electrospun chitosan/PVA nanocomposite nanofibers for biomedical applications. RSC Advances, **5**, 10479–10487 (2015). https://doi.org/10.1039/c4ra13972k

[45] Hotaling N. A., Bharti K., Kriel H., Simon C. G.: DiameterJ: A validated open source nanofiber diameter measurement tool. Biomaterials, **61**, 327–338 (2015). https://doi.org/10.1016/j.biomaterials.2015.05.015

[46] Lopresti F., Pavia F. C., Vitrano I., Kersaudy-Kerhoas M., Brucato V., la Carrubba V.: Effect of hydroxyapatite concentration and size on morpho-mechanical properties of PLA-based randomly oriented and aligned electrospun nanofibrous mats. Journal of the Mechanical Behavior of Biomedical Materials, **101**, 103449 (2020). https://doi.org/10.1016/j.jmbbm.2019.103449

[47] Llana-Ruiz-Cabello M., Pichardo S., Bãnos A., Núñez C., Bermúdez J. M., Guillamón E., Aucejo S., Cameán A. M.: Characterisation and evaluation of PLA films containing an extract of *Allium* spp. to be used in the packaging of ready-to-eat salads under controlled atmospheres. LWT – Food Science and Technology, **64**, 1354–1361 (2015). https://doi.org/10.1016/j.lwt.2015.07.057

[48] Ramos M., Jiménez A., Peltzer M., Garrigós M. C.: Characterization and antimicrobial activity studies of polypropylene films with carvacrol and thymol for active packaging. Journal of Food Engineering, **109**, 513–519 (2012). https://doi.org/10.1016/j.jfoodeng.2011.10.031

[49] Lopresti F., Campora S., Tirri G., Capuana E., Pavia F. C., Brucato V., Ghersi G., la Carrubba V.: Core-shell PLA/Kef hybrid scaffolds for skin tissue engineering applications prepared by direct kefiran coating on PLA electrospun fibers optimized *via* air-plasma treatment. Materials Science and Engineering: C, **127**, 112248 (2021). https://doi.org/10.1016/j.msec.2021.112248

[50] Altan A., Aytac Z., Uyar T.: Carvacrol loaded electrospun fibrous films from zein and poly(lactic acid) for active food packaging. Food Hydrocolloids, **81**, 48–59 (2018). https://doi.org/10.1016/j.foodhyd.2018.02.028

[51] Beachley V., Wen X.: Effect of electrospinning parameters on the nanofiber diameter and length. Materials Science and Engineering: C, **29**, 663–668 (2009). https://doi.org/10.1016/j.msec.2008.10.037

[52] Miletić A., Pavlić B., Ristić I., Zeković Z., Pilić B.: Encapsulation of fatty oils into electrospun nanofibers for cosmetic products with antioxidant activity. Applied Sciences, **9**, 2955–2967 (2019). https://doi.org/10.3390/app9152955

[53] Zhang W., Huang C., Kusmartseva O., Thomas N. L., Mele E.: Electrospinning of polylactic acid fibres containing tea tree and manuka oil. Reactive and Functional Polymers, **117**, 106–111 (2017). https://doi.org/10.1016/j.reactfunctpolym.2017.06.013

[54] Batista R. A., Espitia P. J. P., de Souza Siqueira Quintans J., Freitas M. M., Cerqueira M. Â., Teixeira J. A., Cardoso J. C.: Hydrogel as an alternative structure for food packaging systems. Carbohydrate Polymers, **205**, 106–116 (2019). https://doi.org/10.1016/j.carbpol.2018.10.006

[55] Unalan I., Slavik B., Buettner A., Goldmann W. H., Frank G., Boccaccini A. R.: Physical and antibacterial properties of peppermint essential oil loaded poly(ε-caprolactone) (PCL) electrospun fiber mats for wound healing. Frontiers in Bioengineering and Biotechnology, **7**, 346 (2019). https://doi.org/10.3389/fbioe.2019.00346

[56] Zehetmeyer G., Meira S. M. M., Scheibel J. M., de Brito da Silva C., Rodembusch F. S., Brandelli A., Soares R. M. D.: Biodegradable and antimicrobial films based on poly(butylene adipate-*co*-terephthalate) electrospun fibers. Polymer Bulletin, **74**, 3243–3268 (2017). https://doi.org/10.1007/s00289-016-1896-8

[57] Echeverría C., Limón I., Muñoz-Bonilla A., Fernández-García M., López D.: Development of highly crystalline polylactic acid with β-crystalline phase from the induced alignment of electrospun fibers. Polymers, **13**, 2860 (2021). https://doi.org/10.3390/polym13172860

[58] Neto W. A. R., Pereira I. H. L., Ayres E., de Paula A. C. C., Averous L., Góes A. M., Oréfice R. L., Bretas R. E. S.: Influence of the microstructure and mechanical strength of nanofibers of biodegradable polymers with hydroxyapatite in stem cells growth. Electrospinning, characterization and cell viability. Polymer Degradation and Stability, **97**, 2037–2051 (2012). https://doi.org/10.1016/j.polymdegradstab.2012.03.048

[59] Qin Y., Li W., Liu D., Yuan M., Li L.: Development of active packaging film made from poly(lactic acid) incorporated essential oil. Progress in Organic Coatings, **103**, 76–82 (2017). https://doi.org/10.1016/j.porgcoat.2016.10.017

[60] Scaffaro R., Lopresti F.: Processing, structure, property relationships and release kinetics of electrospun PLA/carvacrol membranes. European Polymer Journal, **100**, 165–171 (2018). https://doi.org/10.1016/j.eurpolymj.2018.01.035

[61] Dheraprasart C., Rengpipat S., Supaphol P., Tattiyakul J.: Morphology, release characteristics, and antimicrobial effect of nisin-loaded electrospun gelatin fiber mat. Journal of Food Protection, **72**, 2293–2300 (2009). https://doi.org/10.4315/0362-028X-72.11.2293

[62] Stramarkou M., Oikonomopoulou V., Missirli T., Thanassoulia I., Krokida M.: Encapsulation of rosemary essential oil into biodegradable polymers for application in crop management. Journal of Polymers and the Environment, **28**, 2161–2177 (2020). https://doi.org/10.1007/s10924-020-01760-5

[63] Rehman A., Tong Q., Jafari S. M., Assadpour E., Shehzad Q., Aadil R. M., Iqbal M. W., Rashed M. M. A., Mushtaq B. S., Ashraf W.: Carotenoid-loaded nanocarriers: A comprehensive review. Advances in Colloid and Interface Science, **275**, 102048 (2020). https://doi.org/10.1016/j.cis.2019.102048

[64] Goldberg M., Langer R., Jia X.: Nanostructured materials for applications in drug delivery and tissue engineering. Journal of Biomaterials Science, Polymer Edition, **18**, 241–268 (2007). https://doi.org/10.1163/156856207779996931

[65] Tampau A., González-Martinez C., Chiralt A.: Carvacrol encapsulation in starch or PCL based matrices by electrospinning. Journal of Food Engineering, **214**, 245–256 (2017). https://doi.org/10.1016/j.jfoodeng.2017.07.005

[66] Tampau A., González-Martínez C., Chiralt A.: Polyvinyl alcohol-based materials encapsulating carvacrol obtained by solvent casting and electrospinning. Reactive and Functional Polymers, **153**, 104603 (2020). https://doi.org/10.1016/j.reactfunctpolym.2020.104603

[67] Han D., Sherman S., Filocamo S., Steckl A. J.: Long-term antimicrobial effect of nisin released from electrospun triaxial fiber membranes. Acta Biomaterialia, **53**, 242–249 (2017). https://doi.org/10.1016/j.actbio.2017.02.029

[68] Li M., Yu H., Xie Y., Guo Y., Cheng Y., Qian H., Yao W.: Fabrication of eugenol loaded gelatin nanofibers by electrospinning technique as active packaging material. LWT, **139**, 110800 (2021). https://doi.org/10.1016/j.lwt.2020.110800

[69] Peppas N. A., Sinclair J. L.: Anomalous transport of penetrants in glassy polymers. Colloid and Polymer Science, **261**, 404–408 (1983). https://doi.org/10.1007/BF01418213

[70] Hogg S.: Essential microbiology. Wiley, Chichester (2013).